SECED 2023 Conference
Earthquake Engineering & Dynamics for a Sustainable Future
14-15 September 2023, Cambridge, UK

OPTIMAL INFRASTRUCTURE DESIGN IN GROWING CITIES: A PEOPLE-CENTERED RISK-INFORMED AND (POSSIBLY) HOLISTIC APPROACH

Fabrizio NOCERA[1] & Gemma CREMEN[2]

Abstract: *The well-being and economic prosperity of societies rely on large-scale interdependent infrastructure and their provision of essential services. However, past events around the world (including major earthquakes) have highlighted the notable vulnerability of infrastructure to natural/anthropogenic hazards, which has had significant societal consequences. Previous research has focused on developing risk-modelling approaches and computational tools for quantifying the consequences of hazardous events on critical infrastructure in urban environments. However, in the context of climate change, rapid population growth, and increasingly interconnected urbanisation, a theoretical framework for designing risk-informed critical infrastructure from a forward-looking, dynamic, and people-centred perspective is required. Although, it is also important to consider that optimising infrastructure design accounting only for natural-hazard risk could have additional (potentially negative) socioeconomic consequences not represented in conventional natural-hazard risk-modelling approaches. In response to these challenges, this paper presents a people-centred, risk-informed decision-making framework for future urban infrastructure development in growing cities. The framework captures the performance of infrastructure in terms of serving the community's needs; the underlying optimal infrastructure design balances this performance in regular conditions, in the immediate aftermath of a hazard, and during the long-term recovery process. We also illustrate a potential expansion of the framework, which involves integrating a bespoke agent-based model that accounts for the implications of variations in infrastructure development on land values and resulting dynamic residential location choices. This final feature of the framework would allow for measuring gentrification, a macro-scale unintended effect of risk-informed infrastructure design that is not explicitly related to natural-hazard events. We demonstrate the framework by optimising the transportation infrastructure design of a hypothetical future community.*

Introduction

Critical infrastructure is vulnerable to natural and anthropogenic hazards (including earthquakes), which can result in significant indirect consequences to communities that are many times larger than the direct costs of infrastructure repair (e.g., Zhang et al. 2020). Numerous previous studies have focused on developing engineering tools to model the consequences of hazards on critical infrastructure in urban environments. For instance, past work has simulated the seismic performance of individual infrastructure components like bridges (e.g., Nocera et al. 2022) and translated earthquake damage to these components into changes in infrastructure functionality (e.g., Nocera et al. 2019). While these tools help to identify vulnerabilities and risks associated with current infrastructure, there is a need for new risk-modelling approaches that inform decision-making around designing disaster-resilient infrastructure (Cremen et al. 2022a). Furthermore, in the context of climate change, rapid population growth, and increasingly interconnected urbanisation, these approaches must use a dynamic, forward-looking, and people-centred perspective, accounting for appropriate uncertainties (Cremen et al. 2022b; Filippi et al. 2023). However, optimising infrastructure design purely in terms of hazard-induced impacts could have additional unintended socioeconomic consequences (e.g., gentrification or population segregation), which are not considered in conventional hazard-related risk-modelling approaches. This means that a so-called risk-informed infrastructure design may end up pricing low-income residents out of their homes and creating urban enclaves, for instance (e.g., Bagheri-Jebelli et al. 2021).

[1] Postdoctoral Research Fellow, University College London, London, UK, f.nocera@ucl.ac.uk
[2] Lecturer, University College London, London, UK

Towards addressing these challenges, we illustrate a people-centred, risk-informed decision-making framework for urban infrastructure development. The framework quantifies the (uncertain) ability of infrastructure to serve a community's needs, using an optimisation procedure to balance its performance in business-as-usual conditions (i.e., before the occurrence of a hazard), in the immediate aftermath of a (future) hazard event (e.g., major earthquake), and during the long-term post-hazard recovery process, accounting for specific end-user priorities across time. In addition, we discuss how the framework could be easily extended to incorporate unintended consequences of optimal risk-informed infrastructure performance. This extension would include a bespoke agent-based model (ABM) that accounts for the implications of infrastructure development on land values and resulting dynamic residential location decision-making. The final infrastructure design would then (i) maximise the natural-hazard (e.g., earthquake) risk-informed performance of the infrastructure; while (ii) limiting unintended socioeconomic consequences to a pre-determined, end-user-specific acceptable level.

Mathematical modelling of infrastructure performance

This section reviews the general mathematical formulation for modelling infrastructure performance based on graph theory (Nocera et al. 2019; Sharma and Gardoni 2022). Networks are defined as a graph $G = (V, E)$ that includes attributes such as names, types, and state variables, as well as the topological information represented by the vertices V and edges E (Sharma and Gardoni 2022).

Following Sharma and Gardoni (2022), we model infrastructure as a collection of networks, each representing a specific function. The collection of all networks is $\mathcal{G} = \{G^{[k]} = (V^{[k]}, E^{[k]}): k = 1, \dots, K\}$, where superscript $[k]$ denotes the function captured by the k^{th} network. Then, the state of each network is characterised by a unique set of vectors: (i) capacity measures $\mathbf{C}^{[k]}(t)$; (ii) demand measures $\mathbf{D}^{[k]}(t)$; and (iii) supply measures $\mathbf{S}^{[k]}(t)$. The triplet $[\mathbf{C}^{[k]}(t), \mathbf{D}^{[k]}(t), \mathbf{S}^{[k]}(t)]$ is used to compute an overall performance measure $\mathbf{Q}^{[k]}(t)$ of $G^{[k]}$. Network measures are a function of dynamic state variables $\mathbf{x}^{[k]}(t)$, where the temporal dependence accounts for deterioration/ageing processes (e.g., Jia and Gardoni 2018) or recovery activities (e.g., Sharma et al. 2020). To capture the time-dependent performance of infrastructure across a region, we define an aggregated measure $Q(t)$ of the component performances $\mathbf{Q}^{[k]}(t)$. Then, $\mathfrak{R}[Q(t)]$ denotes some specific societal benefit of infrastructure performance. $\mathfrak{R}[Q(t)]$ can be disaggregated based on socioeconomic factors (e.g., income, age, gender) to capture higher resolution effects of infrastructure performance (or non-performance) across diverse sections of the population.

Proposed framework

This section presents the framework for facilitating people-centred, risk-informed infrastructure design. We formulate infrastructure design as a combinatorial optimisation problem, aiming to maximise overall infrastructure performance across three temporal phases – i.e., (i) business-as-usual operations; (ii) in the immediate aftermath of a hazard event (i.e., the response phase); and (iii) during long-term recovery efforts (i.e., the recovery phase) - that are prioritised according to end-user input.

Mathematical formulation of the optimisation

We write the objective function Z of the optimisation problem as

$$\max Z = \mathbb{E}[(\gamma_1 \cdot Z_1 + \gamma_2 \cdot Z_2 + \gamma_3 \cdot Z_3)] \quad (1)$$

where $\mathbb{E}[\cdot]$ is the expected value operator; γ_1, γ_2, and γ_3 are weights, respectively defining the end-user-dependent relative importance of infrastructure performance during the business-as-usual, response, and recovery phases; and Z_1, Z_2, and Z_3 represent infrastructure performance in the corresponding phases. Z_1 is formulated as

$$Z_1 = \frac{1}{n_a}\sum_{a=1}^{n_a} \omega_a \frac{1}{N_H}\sum_{i=1}^{N_H} w_i \mathfrak{R}_{i,a}[Q(t_{0^-}; \mathbf{g})] \quad (2)$$

where n_a is the number of considered infrastructure needs (e.g., locations/activities required to be accessed by a transportation infrastructure), ω_a is the weight (priority) placed on the a^{th} infrastructure need, N_H is the number of household agents in the community, and w_i is the weight (priority) placed on meeting the i^{th} household's infrastructure needs. $\mathfrak{R}_{i,a}[Q(t_{0^-},\mathbf{g})]$ describes a specific benefit of infrastructure performance at household-level during t_{0^-} (before the occurrence of the hazard event) and $\mathbf{g}$ is the set of $E^{[k]}$ to be added as part of the infrastructure development, such that different $G^{[k]}$ will result in different values of $\mathfrak{R}_{i,a}[Q(t_{0^-};\mathbf{g})]$. In the example case of using a topology-based approach to measure the performance of a transportation infrastructure, we can define $\mathfrak{R}_{i,a}[Q(t_{0^-},\mathbf{g})]$ as

$$\mathfrak{R}_{i,a}[Q(t_{0^-},\mathbf{g})] = \frac{\eta_{i,a}^{(H)}(t_{0^-},\mathbf{g})}{\eta_{i,a}^{*}(t_{0^-},\mathbf{g})} = \\ = \frac{1}{N(i)}\sum_{m=1}^{N(i)} \frac{d_{i,a(m)}^{*}}{d_{i,a(m)}} \tag{3}$$

where $N(i)$ is the number of individuals in household i that have infrastructure need a to access a given location of interest, $d_{i,a(m)}$ is the distance from the residence of household agent i to the location of interest of the m^{th} individual in household i, and $d_{i,a(m)}^{*}$ is a reference value for normalising $d_{i,a(m)}$ (e.g., the maximum value of $d_{i,a(m)}$ within the corresponding socioeconomic group) so that each component of the objective function in Eq. (1) can be added together. Z_2 is expressed as

$$Z_2 = \frac{1}{n_{a'}}\sum_{a'=1}^{n_{a'}} \omega_{a'} \frac{1}{N_H} \sum_{\substack{i=1,\\ p(i)\subseteq i\in\Omega_{a'}}}^{N_H} w_i \mathfrak{R}_{i,a'}[Q(t_{0^+}),\mathbf{g}] \tag{4}$$

where $\omega_{a'}$ is the weight associated with the a'^{th} infrastructure need in the response phase t_{0^+}, $p(i) \subseteq i \in \Omega_{a'}$ identifies the individuals (in household i) associated with the a'^{th} infrastructure need in the response phase, and $\mathfrak{R}_{i,a'}[Q(t_{0^+},\mathbf{g})]$ describes some benefit of infrastructure performance in the response phase. In the context of using a topology-based approach to measure the performance of a transportation infrastructure, we can define $\mathfrak{R}_{i,a'}[Q(t_{0^+},\mathbf{g})] = \eta_{i,a'}^{(H)}(t_{0^+},\mathbf{g})/\eta_{i,a'}^{(H)}(t_{0^-},\mathbf{g})$, capturing the increase in distance to each location of interest at the household level compared to those distances at t_{0^-}. The locations of interest captured by $\mathfrak{R}_{i,a'}[Q(t_{0^+},\mathbf{g})]$ may be different to those captured by $\mathfrak{R}_{i,a}[Q(t_{0^-},\mathbf{g})]$ in Eq. (3), and could be limited to shelters (for those who are displaced) and hospitals (for those who are injured), for instance. Finally, Z_3 is expressed as

$$Z_3 = \frac{1}{T_R}\sum_{\tau=t_{0^+}}^{T_R} \frac{1}{n_a}\sum_{a=1}^{n_a} \omega_a \frac{1}{N_H}\sum_{i=1}^{N_H} w_i \mathfrak{R}_{i,a}[Q(\tau,\mathbf{g})] \tag{5}$$

where T_R represents the time at which recovery activities are completed, and $\mathfrak{R}_{i,a}[Q(\tau,\mathbf{g})]$ is a time-varying measure of some benefit of infrastructure performance during the recovery process. Considering a topology-based approach to measuring performance of a transportation infrastructure, we can define $\mathfrak{R}_{i,a}[Q(\tau,\mathbf{g})] = \eta_{i,a}^{(H)}(t,\mathbf{g})/\eta_{i,a}^{(H)}(t_{0^-},\mathbf{g})$ analogous to $\mathfrak{R}_{i,a'}[Q(t_{0^+},\mathbf{g})]$ in Eq. (4), where the locations of interest are the same as those captured by $\mathfrak{R}_{i,a}[Q(t_{0^-},\mathbf{g})]$ in Eq. (3).

The first constraint of the optimisation is

$$C_p \leq M_p \tag{6}$$

where C_p is the cost of implementing a specific infrastructure design, and M_p is the budget allocated to the infrastructure development process. We also force the resulting $G^{[k]}$ to be a connected network, which can be written as

$$\forall v_1, v_2 \in V^{[k]}, \exists\ \varphi(v_1,v_2) \tag{7}$$

where v_1 and v_2 are two generic nodes in $V^{[k]}$, and $\varphi(v_1,v_2)$ is a path between them. We include additional non-negative constraints $\omega_a \geq 0, \forall a$, $w_i \geq 0, \forall i$, $\omega_{a'} \geq 0, \forall a'$, and $\gamma_1,\gamma_2,\gamma_3 \geq 0$, and ensure that sets of weights ω_a, w_i, $\omega_{a'}$, and γ_1, γ_2 and γ_3 sum to one. The final constraint of the optimisation is $\eta_{i,a}^{(H)}(\tau^*,\mathbf{g})/\eta_{i,a}^{(H)}(t_{0^-},\mathbf{g}) \geq \xi(\tau^*), \forall\tau^*$, where $\xi(\tau^*)$ represents a lower threshold for infrastructure performance at time τ^*, facilitating a possible requirement for the infrastructure to be restored to pre-hazard performance levels within a certain timeframe.

Solving for the final infrastructure design

The optimal infrastructure layout (topology) results from a finite set of possible infrastructure interventions, i.e., added edges, such as new roads in a transportation infrastructure. We start with an augmented infrastructure layout that includes the existing infrastructure components and the full set of potential (candidate) edges for development. Several procedures can be used to obtain the augmented layout, such as (i) manually digitising the candidate edges in a geographic information system; (ii) defining a grid of points based on digitised geospatial data in a geographic information system and finding the least cost paths among all the points in the grid; or (iii) using a fully-automated interactive procedural modelling approach based on tensor field theory (e.g., Chen et al. 2008). First, we find the combination of new edges to be added that maximises the objective function in Eq. (1) and satisfies the constraints of the optimisation problem discussed in the previous section.

An exhaustive search of every possible combination of new edges is not feasible because of several computational complexities, such as nonlinearity, non-convexity, and non-differentiability of the objective function in Eq. (1). However, heuristic approaches can be used to obtain near-optimal solutions, and we use a simulated annealing (SA)-based metaheuristic procedure in our framework. SA-based heuristics maximise/minimise an objective function by applying small random changes to the decision variable $\mathbf{g}$, i.e., the edges to add from the full set of candidates. If a new solution improves the value of the objective function, a further search is initiated in the neighbourhood of this point to determine a solution that further improves the objective function. If a further solution cannot be found, the current solution is accepted with a certain probability, i.e., $\exp(-Z/T)$, in which Z is the objective function in Eq. (1), and T is one of the hyperparameters of the optimisation algorithm, typically known as the temperature.

We start the search for the optimal infrastructure layout by randomly selecting a subset of candidate edges that satisfy the constraints of the optimisation problem. We evaluate the objective function using this subset as the initial optimisation solution. Then, the initial solution is perturbed by making small changes to the current subset of candidates. For each perturbation, we randomly select one of the following options: *add*, *remove*, or *replace*. If *add* is selected, we randomly add a new edge candidate from the full set of candidates to the current subset. If *remove* is selected, we randomly remove a candidate from the current subset. If *replace* is selected, we randomly replace a candidate from the current subset with a new candidate from the full set of candidates.

Next, we avoid infeasible solutions that violate the constraints of the optimisation problem by adding a dynamic penalty function (Michalewicz and Schoenauer 1996) to the solution of the objective function. Mathematically, this means that we rewrite Eq. (1) as

$$Z' = \begin{cases} Z & \text{if } \mathbf{g} \in \Omega_f \\ Z + P(\mathbf{g}) & \text{otherwise} \end{cases} \tag{8}$$

where Ω_f is the set of feasible solutions, and the penalty function $P(\mathbf{g})$ is introduced if there is a violation of the constraints of the optimisation problem. Following Michalewicz and Schoenauer (1996), $P(\mathbf{g})$ can be expressed as $P(\mathbf{g}) = (1/2T) \cdot [Y(\mathbf{g})^2]$, where $Y(\mathbf{g})$ is a constraint of Z, and all other variables are as previously defined. The optimisation result is a sorted list of infrastructure development layouts ranked in terms of the value of the objective function in Eq. (1).

A participatory, people-centred process

The illustrated framework is inherently participatory in nature. Infrastructure needs a and a' can be identified through discussions with affected communities, ensuring that the infrastructure development process is based on local people's requirements. Values of γ_1, γ_2, γ_3, ω_a, and $\omega_{a'}$ should be defined by relevant (local) decision-makers. Values of w_i can be assigned based on socioeconomic characteristics such as income, which can help to prioritise the needs of lower-income populations and support a pro-poor approach (e.g., Galasso et al. 2021).

Illustrative example

This section demonstrates the proposed framework for designing an expansion of the roadway transportation infrastructure of the Futureville virtual urban testbed to accommodate expected infrastructure needs associated with future urbanisation, i.e., when all zones of Futureville are inhabited (Cremen et al. 2022a). Futureville is a geospatial database of urban features that includes buildings and infrastructure. It contains social information on resident households (such as income levels) and individuals, as well as detailed data on each person's daily infrastructure needs. The testbed is a heavily altered version of the Centerville Virtual Community presented in Ellingwood et al. (2016). It was developed on the same physical footprint as Centerville (located in the Midwestern U.S.) but contains a modified set of engineering assets, details of which can be found in Cremen et al. (2022a). However, the initial roadway transportation infrastructure of Futureville is identical to that of Centerville.

The hazard event considered is a hypothetical earthquake with magnitude $M_w = 7.9$ and a depth of 10 km, located 25 km southwest of Futureville. The map of the Peak Ground Acceleration (PGA) at the site of the vulnerable components considered in this paper, i.e., bridges, is obtained from the Fernandez and Rix (2006) ground-motion model (GMM), which is valid for the hypothetical location of Futureville. This GMM characterises PGA as a function of magnitude and epicentral distance. Since this is purely an illustrative demonstration of the framework, we only consider the median values of PGA determined from the GMM.

We use bridge fragility functions detailed in Nielson and DesRoches (2007) – which are appropriate for the hypothetical location of Futureville – to obtain the probability of each bridge being in a particular damage state, considering slight, moderate, extensive, and complete damage states. Table 1 summarises the bridge types included in the current and potential future roadway transportation infrastructure of Futureville.

Bridge (see Figure 1)	**Bridge type**	**Abbreviation (Nielson and DesRoches 2007)**
B1	Multispan continuous concrete girder	MSC concrete
B2	Multispan continuous slab	MSC slab
B3	Multispan continuous steel girder	MSC steel
B4	Multispan simply supported concrete box girder	MSSS conc box
B5	Multispan simply supported concrete girder	MSSS concrete
B6	Multispan simply supported slab	MSSS slab
B7	Single span steel girder	SS steel
B8	Multispan simply supported steel girder	MSSS steel
B9	Single span steel girder	SS steel
B10	Single span concrete girder	SS concrete
B11	Single span concrete girder	SS concrete
B12	Single span concrete girder	SS concrete

Table 1. Bridge types that feature in the current and potential future roadway transportation infrastructure of Futureville.

Then, we quantify the performance of the transportation infrastructure during business-as-usual operations t_{0^-} and the response phase t_{0^+} (i.e., $\gamma_3 = 0$), assuming that the infrastructure needs include access to hospitals (h) and workplaces (l) in both temporal phases, i.e., $a = a' = \{h, l\}$. In this example, we assume there is one hospital located in Zone 4 (a retail/business zone), see Figure 1. We estimate $\mathfrak{R}_{i,a}[Q(t_{0^-}, \mathbf{g})]$ and $\mathfrak{R}_{i,a'}[Q(t_{0^+}, \mathbf{g})]$ using a topology-based approach and assuming a bridge is closed when its damage state is at least moderate (Nocera et al. 2019).

We make the following additional assumptions: (i) $\gamma_1 = \gamma_2 = 0.5$, (ii) $\boldsymbol{\omega}_a = \boldsymbol{\omega}_{a'} = [1/2\,, 1/2]$ for households with at least one employed individual and $\boldsymbol{\omega}_a = \boldsymbol{\omega}_{a'} = [1{,}0]$ for retired households. The assumed weights reflect an objective stakeholder who places equal importance on each temporal phase and infrastructure need when making decisions; (iii) $\mathbf{w}_i = [0.7, 0.2, 0.1]$, where the vector entries respectively refer to low-income, middle-income, and high-income households, reflecting stakeholders that adopt a pro-poor approach.

Figure 1 displays the augmented transportation infrastructure layout of Futureville, where the existing transportation infrastructure is indicated in black.

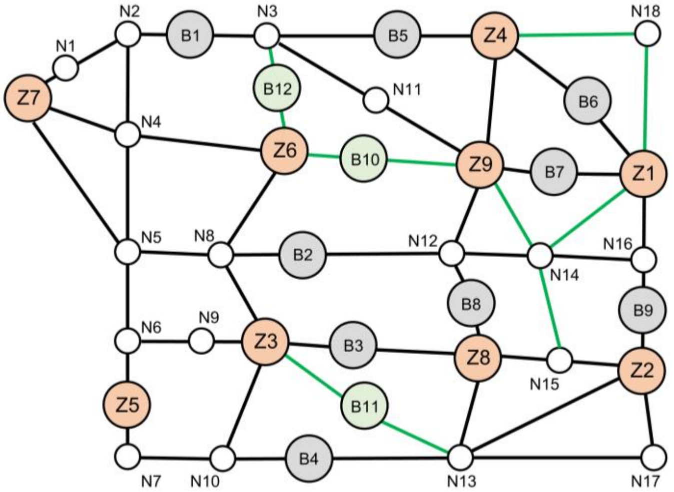

Figure 1. Case-study application. Z corresponds to a zone, B to a bridge, and N to a generic node.

The full set of candidate edges is shown in green, which we obtain through a manual digitisation process that hypothetically reflects the outcome of a conversation with potential stakeholders. Table 2 summarises the assumed costs of building the new roads in Figure 1. We investigate three possible budgets that would be available to stakeholders for the infrastructure development, i.e., M_p = £ 10M, £ 37.5M, and £ 50M.

New road	**Cost (in millions)**
N3-B12	£ 5
B12-Z6	£ 5
Z6-B10	£ 10
B10-Z9	£ 10
Z3-B11	£ 7.5
B11-N13	£ 7.5
Z4-N18	£ 2.5
N18-Z1	£ 2.5
Z9-N14	£ 2.5
Z1-N14	£ 2.5
N14-N15	£ 2.5

Table 2. Assumed construction costs of new roads.

Figure 2 displays the final infrastructure designs associated with the three considered budget scenarios, where the added edges are shown in blue.

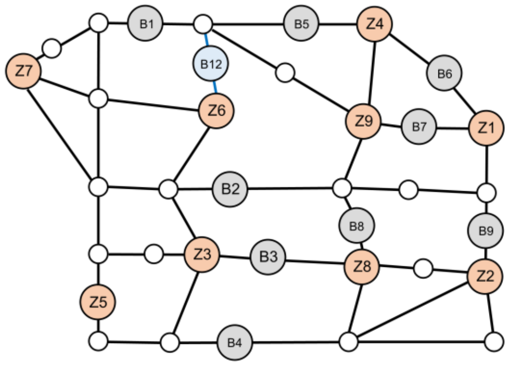

(a) $M_p = £\ 10\mathrm{M}$

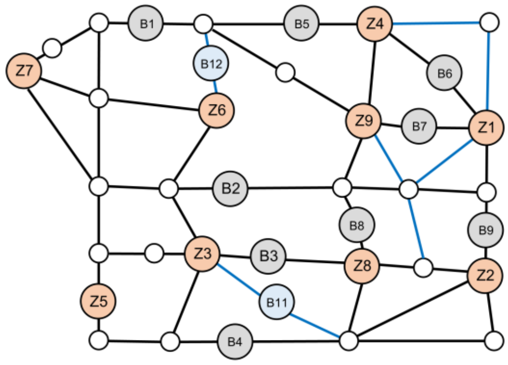

(b) $M_p = £\ 37.5\mathrm{M}$

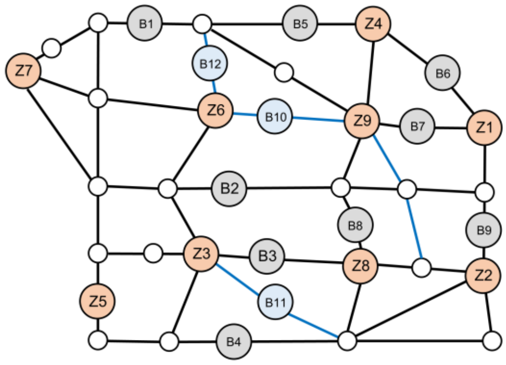

(c) $M_p = £\ 50\mathrm{M}$

Figure 2. Infrastructure layout development for the three considered budget scenarios, where the added edges are shown in blue.

The results show that the value of Z improves by 10%, 14.5%, and 14.6% for the three budget scenarios, respectively, compared to the Z obtained for the initial transportation infrastructure. Furthermore, investing $£\ 10\mathrm{M}$ is enough to ensure that all households of Futureville will have access to the hospital (located in Zone 4) after the earthquake.

Agent-based modelling of unintended consequences

We now discuss how the proposed framework could be extended to incorporate unintended consequences of optimal risk-informed infrastructure performance through a bespoke ABM, capturing the implications of infrastructure development on land values and resulting dynamic residential location decision-making (e.g., Alonso 1964). The ABM features buyer and seller agents interacting with a spatial context of residential units. The benefit gained by an agent from a residential unit is quantified using utility values, which depend on the agent's preferences towards various related attributes that depend on the state of infrastructure provision (e.g., proximity to locations that correspond with infrastructure needs). Buyers relocate to maximise utility within the limits of their available budget (e.g., Magliocca et al. 2014).

Mathematically, we write the utility of a residential unit as

$$U_{r,i} = \sum_{j=1}^{n} \alpha_{i,j} \cdot u(\lambda_j) \tag{9}$$

where $U_{r,i}$ is the total utility of residential unit r for the i^{th} agent, $\alpha_{i,j}$ is the weight representing the preference of the i^{th} agent towards attribute λ_j, $u(\lambda_j)$ is the utility associated with the j^{th} attribute, and n is the number of attributes. We write $u(\lambda_j)$ as

$$u(\lambda_j) = \begin{cases} \dfrac{\lambda_j}{\max(\lambda_j)} & \text{if } \lambda_j \in \Lambda \\ 1 - \dfrac{\lambda_j}{\max(\lambda_j)} & \text{otherwise} \end{cases} \tag{10}$$

where Λ is the set of desirable attributes. Next, we distinguish between agents as either buyers, b, or sellers, s, i.e., $i \in \{b, s\}$. We write the b^{th} buyer's willingness to pay for the r^{th} residential unit $WTP_{r,b}$, as

$$WTP_{r,b} = \frac{H_b \cdot U_{r,b}^2}{\beta_b + U_{r,b}^2} \tag{11}$$

where H_b is the b^{th} buyer's available budget, and β_b is a parameter controlling the convexity of $WTP_{r,b}$, reflecting the risk appetite of the buyer. The range of β_b is the same as that of $U_{r,b}$; high β_b indicates risk-averse behaviour and low β_b indicates risk-taking behaviour. We write the price of the r^{th} residential unit set by the s^{th} seller, $P_{r,s}$ as

$$P_{r,s} = \frac{H_s . U_{r,s}^2}{\beta_s + U_{r,s}^2} \tag{12}$$

where H_s is the expected budget of the buyer, and β_s is analogous to β_b .

Modelling details

The ABM captures the behaviour of household agents in the form of a relocation action. Relocation occurs for the b^{th} household buyer agent when $P_{r,s} > WTP_{r,b}$. Relocating households move to the first residential unit r^* (within a set of θ residential units in their current neighbourhood) that satisfies (i) $WTP_{r,b} \geq P_{r,s}$ and (ii) $U_{r,b} \geq U_b^*$, where U_b^* is a utility threshold equal to the average utility value of the θ residential units. If none of the θ residential units meet these conditions, the household instead emigrates out of the urban system. Thus, relocations are triggered by changes in $P_{r,s}$ and/or $WTP_{r,b}$; these result from changes to λ_j that arise from infrastructure development. Unintended consequences of infrastructure development are quantified in terms of the total number of triggered relocations ε (i.e., the number of times $P_{r,s} > WTP_{r,b}$ is valid for household buyer agents). In summary, ε can be thought of as forced evictions, which are a proxy for gentrification.

Integrating unintended consequences in the risk-informed infrastructure development framework

The risk-informed design process previously introduced could further consider the tolerable level of unintended consequences ε resulting from the infrastructure layout, through the workflow presented in Figure 3. In this case, the optimisation result stored would be a sorted list of infrastructure development layouts ranked in terms of the value of the objective function in Eq. (1) (referred to as the "optimised infrastructure set" in Figure 3). Then, the final infrastructure layout selected would be the one ranked highest in the optimisation set that yields $\varepsilon \leq \varepsilon_T$, where ε_T is a pre-determined, end-user-specific acceptable level of unintended gentrification.

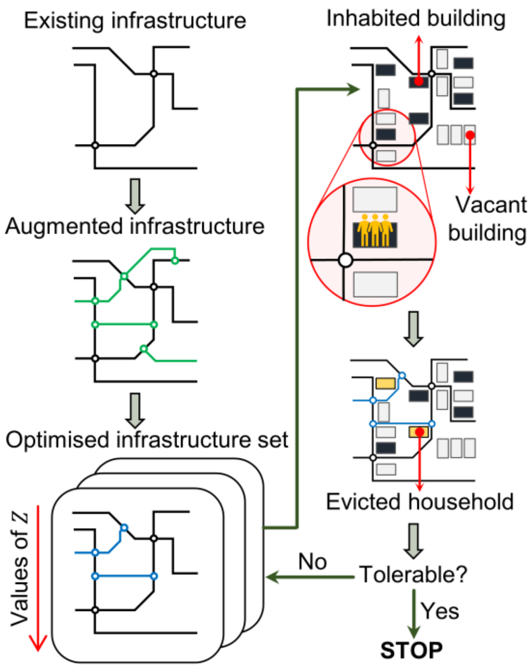

Figure 3. Workflow for finding the final infrastructure design, accounting for the unintended consequence of gentrification.

Conclusions

This paper illustrated a people-centred, risk-informed decision-making framework for future infrastructure development in growing cities. We formulated the risk-informed infrastructure development process as a combinatorial optimisation problem, in which the objective is to maximise the performance of the infrastructure in three distinct temporal phases, i.e., business-as-usual conditions, in the immediate aftermath of a (future) hazard, and during the long-term recovery process, according to stakeholder/end-user priorities and needs. We applied the framework to optimise the transportation infrastructure design of a hypothetical future community.

This example application revealed that different investments in infrastructure lead to varying levels of improvement in accessibility (as expected), although the benefits do not increase linearly with expenditure. It was also found that accessibility to essential services (i.e., hospitals) after the occurrence of a (future) earthquake could be achieved using a limited budget (the lowest one investigated).

In addition, we illustrated how the framework could be extended to incorporate unintended consequences of optimal risk-informed infrastructure performance through a bespoke agent-based model (ABM) that accounts for the implications of infrastructure development on land values and resulting dynamic residential location decision-making. If unintended consequences of risk-informed infrastructure design are also considered, the final infrastructure design selected would be the one that (i) maximises the performance of the infrastructure considering the effects of hazard (e.g., earthquake) events; while (ii) limiting unintended socioeconomic consequences to a pre-determined, end-user-specific acceptable level. In summary, the illustrated framework extends beyond conventional natural-hazard infrastructure impact assessments by (i) focusing on future infrastructure design; as well as introducing a design process that (ii) facilitates external participation and (iii) possibly adopts a more holistic lens by explicitly accounting for unintended consequences of risk-informed infrastructure development (e.g., gentrification).

Acknowledgements

This work was supported by the United Kingdom Research and Innovation (UKRI) Global Challenges Research Fund (GCRF) under grant NE/S009000/1, Tomorrow's Cities Hub. The authors are also grateful to Yahya Gamal for helpful discussions and input on material related to the potential agent-based modelling component of the framework.

References

Alonso W (1964), *Location and land use: Toward a general theory of land rent,* Harvard University Press

Bagheri-Jebelli N, Crooks A and Kennedy WG (2021), *Capturing the Effects of Gentrification on Property Values: An Agent-Based Modeling Approach*, In Springer Proceedings in Complexity. Springer International Publishing

Chen G, Esch G, Wonka P, Müller P and Zhang E (2008), Interactive procedural street modeling, *ACM Transactions on Graphics*, 27(3)

Cremen G, Galasso C and McCloskey J (2022a), A Simulation-Based Framework for Earthquake Risk-Informed and People-Centered Decision Making on Future Urban Planning, *Earth's Future*, 10(1): e2021EF002388

Cremen G et al. (2022b), A state-of-the-art decision-support environment for risk-sensitive and pro-poor urban planning and design in Tomorrow's cities, *International Journal of Disaster Risk Reduction*, 103400

Ellingwood BR, Cutler H, Gardoni P, Peacock WG, van de Lindt JW and Wang N (2016), The Centerville virtual community: A fully integrated decision model of interacting physical and social infrastructure systems, *Sustainable and Resilient Infrastructure*, *1*(3-4): 95-107.

Fernández JA and Rix GJ (2006), *Soil attenuation relationships and seismic hazard analyses in the upper Mississippi embayment*. In Proceedings of the 8th US National Conference on Earthquake Engineering, San Francisco, California.

Filippi ME et al. (2023), Interdisciplinarity in practice: Reflections from early-career researchers developing a risk-informed decision support environment for Tomorrow's cities, *International Journal of Disaster Risk Reduction*, 85: 103481

Galasso C et al. (2021), Risk-based, Pro-poor Urban Design and Planning for Tomorrow's Cities, *International Journal of Disaster Risk Reduction*, 58: 102158

Jia G and Gardoni P (2018), State-dependent stochastic models: A general stochastic framework for modeling deteriorating engineering systems considering multiple deterioration processes and their interactions, *Structural Safety*, 72: 99-110

Magliocca NR, Brown DG and Ellis EC (2014), Cross-Site Comparison of Land-Use Decision-Making and Its Consequences across Land Systems with a Generalized Agent-Based Model, *PLoS ONE*, 9(1), e86179

Menteşe E, Cremen G, Gentile R, Galasso C, Filippi ME and McCloskey J (2023), Future exposure modelling for risk-informed decision making in urban planning, *International Journal of Disaster Risk Reduction*, 103651

Michalewicz Z and Schoenauer M (1996), Evolutionary algorithms for constrained parameter optimisation problems, *Evolutionary Computation*, 4(1): 1-32

Nielson BG and DesRoches R (2007), Analytical seismic fragility curves for typical bridges in the central and southeastern United States, *Earthquake spectra*, *23*(3): 615-633

Nocera F, Tabandeh A, Guidotti R, Boakye J and Gardoni P (2019), *Physics-based fragility functions: Their mathematical formulation and use in the reliability and resilience analysis of transportation infrastructure*, In P. Gardoni (Ed.), Routledge handbook of sustainable and resilient infrastructure, Routledge

Nocera F, Tabandeh A and Gardoni P (2022), *Physics-Based Probabilistic Models for the Reliability Analysis of Bridges,* In Proceedings of the 1st Conference of the European Association on Quality Control of Bridges and Structures: EUROSTRUCT 2021, Springer International Publishing

Sharma N, Tabandeh A and Gardoni P (2020), Regional resilience analysis: A multiscale approach to optimise the resilience of interdependent infrastructure, *Computer‐Aided Civil and Infrastructure Engineering*, 35(12): 1315-1330

Sharma N and Gardoni P (2022), Mathematical modeling of interdependent infrastructure: An object-oriented approach for generalised network-system analysis, *Reliability Engineering & System Safety*, 217: 108042

Zhang C, Yao W, Yang Y, Huang R and Mostafavi A (2020), Semiautomated social media analytics for sensing societal impacts due to community disruptions during disasters, *Computer-Aided Civil and Infrastructure Engineering*, 35(12): 1331-1348